Journal of Applied Polymer Science

Smoke suppression properties of epoxy crosslinked structure and intumescent fire retardant in epoxy-based intumescent fire-retardant coating

Pengfei Chen, Feng Zhang, Shaoxiang Li, Yunfei Cheng
College of Environment and Safety Engineering, Qingdao University of Science and Technology, 53 Zhengzhou Road, Qingdao 266042, People's Republic of China
Correspondence to: F. Zhang (E-mail: zhangfengqd@163.com)

ABSTRACT: In this article, the smoke production behaviors of crosslinked epoxy/polyamide resin (EP/PA) and intumescent fire retardant (IFR) in epoxy-based intumescent fire-retardant coating (IFR-EP) have been investigated using cone calorimeter, smoke density instrument, and thermogravimetric analysis and Fourier transform infrared spectroscopic measurement. The static and dynamic smoke production behaviors of EP/PA and IFR-EP indicate that the IFR has an excellent smoke suppression effect on EP/PA by forming protective char layer in the late combustion stage, while the epoxy crosslinked structure in IFR-EP can enhance the thermal stability and reduce smoke production in the early combustion stage. In addition, according to the discussion of pyrolysis gas products, the IFR can effectively suppress the production of toxic and inflammable gases during the combustion process. © 2016 Wiley Periodicals, Inc. J. Appl. Polym. Sci. **2016**, *133*, 43912.

KEYWORDS: coatings; degradation; flame retardance; polyamides; thermogravimetric analysis

Received 12 February 2015; accepted 12 May 2016
DOI: 10.1002/app.43912

INTRODUCTION

With the development of polymeric materials, more and more natural and synthetic polymers have been used in a wide variety of industrial and household products.[1] Epoxy resin (EP) is among the most important materials in modern polymer industries because of its balance of excellent heat, solvent, moisture and chemical resistance, good mechanical and electrical properties, and satisfactory adherence to many substrates.[2–5] Polyamide resin (PA), which is an excellent curing agent for EP, can provide highly crosslinked network, tough and flexible film, and hydrophobicity to the coating. The crosslinked EP/PA, as film former for epoxy-based coating, has good corrosion inhibition performance and adhesion to the substrates.[6] However, the pure EP is easily ignited and releases large quantities of heat, smoke, and even toxic gases during combustion; hence exploring fire and smoke production behaviors of EP has been a hot and challenging issue.[7,8]

The most effective method to reduce fire hazard of polymer is to introduce proper fire-retardant fillers that act by interfering with the radical flame reaction, changing the solid-state degradation mechanism of the polymer and producing a barrier layer (char or glass) to the heat feedback.[9] These modifications generally affect the degradation by interaction at the molecular level. The action of the fire-retardant materials can occur in condensed or vapor phase or in both phases.[10]

Originally, halogen-contained fire retardants such as brominated compounds are the most common fillers to improve the fire retardancy of polymers. However, the utilization of these halogen-contained fire retardants will produce dense smoke and corrosive hydrogen halide, which do great harm to the environmental and public safety.[11,12] Therefore, halogen-free fire retardants have become more popular to improve the fire retardancy of polymers.[13–15] Among the halogen-free fire retardants, phosphorus-based fire retardants have been found to produce less toxic gases and smoke than the halogen-contained fire retardants.[16] In general, phosphorus-based fire retardants influence the flame behaviors of polymers, acting in condensed and gas phases.[17] The most effective phosphorous-based fire retardants are ammonium polyphosphate (APP) and melamine (MEL) pyrophosphate.[18,19] These additives have been used alone or in synergy with other fillers.

Intumescent fire retardant (IFR), an important class of halogen-free fire retardants, is regarded as one of the most promising fire retardants owing to its low smoke emission, low corrosivity, low toxicity, and low heat release properties.[20–22] Moreover, the IFR has been widely used in epoxy-based intumescent fire-retardant

coatings (IFR-EPs), which have outstanding chemical stability, mechanical property, and binding strength.[23] The IFR generally consists of three constituents: inorganic acid sources, blowing agents, and carbon agents. In this article, the IFR-EP was prepared by EP and PA as matrix resins, APP as acid source, MEL as blowing agent, and pentaerythritol (PER) as carbon agent.

According to the previous work, most of studies focus on the fire retardancy of IFR during combustion[24]; little research about smoke suppression properties of epoxy crosslinked structure and IFR in the IFR-EP can be found. However, in most cases of real fire hazards, the dense smoke and toxic substances released by polymer materials are the major factors leading to death.[25] Furthermore, the EP/PA, as the most common film former for IFR coatings, tends to release large amount of smoke and toxic gases during combustion. Thus, exploring smoke production behaviors of EP/PA and IFR-EP is the key to further explore the applications of IFR-EP.

Based on these considerations, this article studies the smoke production behaviors of EP/PA and IFR-EP using cone calorimeter, smoke density instrument, and thermogravimetric (TG) analysis and Fourier transform infrared (FTIR) spectroscopic measurement, and then, the smoke suppression mechanism and pyrolysis gas products of EP/PA and IFR-EP are also considered and discussed.

EXPERIMENTAL

Materials

Commercial EP (E-44) was bought from Sinopec Baling Petrochemical Company, China. PA (low-molecular 650) used as curing agent, was purchased from Zhenjiang Danbao resin Co., Ltd., China. APP (G.R.) was obtained from Qingdao Haida Chemical Co., Ltd., China. PER (A.R.) was supplied by Tianjin Guangfu Chemical Co., Ltd., China. MEL (A.R.) was a product from Shanghai Aibi Chemical Reagent Co., Ltd., China. Dimethylbenzene (DMB, A.R.) used as solvent, was taken from Laiyang economic and technological development zone Fine Chemical Co., Ltd., China.

Sample Preparation

Preparation of EP/PA: EP and PA were heated in a 60 °C water bath for about 20 min, respectively. Then, the EP and PA in the ratio of 3:2 were mixed and the blends were stirred completely and poured into specified size aluminum moulds. At last, all the samples were dried for 2 days at ventilated place.

Preparation of IFR-EP: APP, PER, and MEL in the ratio of 5:3:2 were mixed with EP which was dissolved in DMB, and the mixtures were grinded into ultrafine particles by cone mill. After that the PA dissolved in DMB was added to the mixtures and stirred well. The end mixtures were poured into aluminum molds. Then, all the samples were dried for at least three weeks at ventilated place. Note that the ratio of film former (EP/PA) and IFR system was 1:1.[26]

Measurements

The static smoke production behaviors of resins were characterized using a smoke density instrument (JQSYM-2) according to GB8323.2-2008 and ISO5659.2-2006 with an incident flux of 25 kW m^{-2}. Each sample was put into an aluminum mold; the dimensions of test samples were 75 mm × 75 mm × 2 mm, 75 mm × 75 mm × 4 mm or 75 mm × 75 mm × 6 mm.

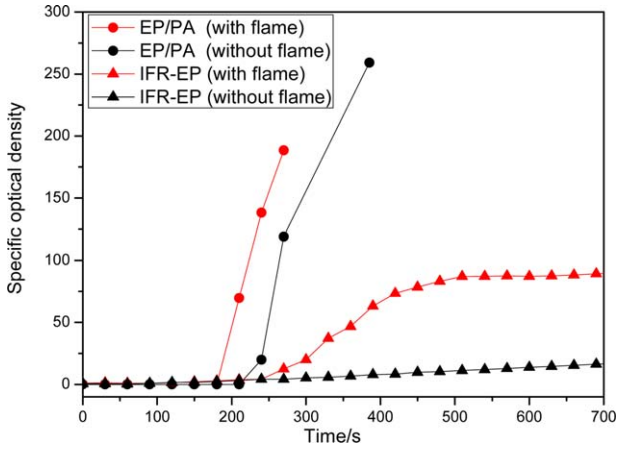

Figure 1. Specific optical density curves of EP/PA and IFR-EP at a flux of 25 kW m^{-2}. [Color figure can be viewed in the online issue, which is available at wileyonlinelibrary.com.]

The cone calorimeter (Stanton Redcroft, UK) tests were performed according to ISO 5660 standard procedures with an incident flux of 35 kW m^{-2} or 50 kW m^{-2}. Each sample was wrapped in aluminum foil, which was then put into the sample holder in the horizontal orientation for testing. The dimensions of test samples were 100 mm × 100 mm × 2 mm, 100 mm × 100 mm × 4 mm or 100 mm × 100 mm × 6 mm.

TG analyses were performed under air flow on a STA 409C TG apparatus (Netzsch Company, Germany) with crucible sample holders, at a heating rate of 20 °C min^{-1}.

FTIR spectra were recorded between 500 and 4000 cm^{-1} with an IR Prestige-21 spectrometer from Shimadzu Corporation, Japan.

RESULTS AND DISCUSSION

Static Smoke Production Behaviors of EP/PA and IFR-EP

To get comprehensive information about the static smoke production behaviors of EP/PA and IFR-EP, the smoke density tests were carried out under different test conditions.

Figure 1 shows the specific optical density (D_s) curves of 2-mm-thick samples at a flux of 25 kW m^{-2} under flame or flameless combustion condition. It can be seen from Figure 1 that the D_s curves of both EP/PA and IFR-EP have lower values without flame, indicating that the combustible materials derived from the degradation will be ignited to generate more smoke. Note that, the D_s values of IFR-EP are much lower than that of EP/PA under whether flame or flameless combustion condition, suggesting that the IFR can effectively suppress the production of smoke and toxic gases.

Figure 2(a) shows the 4-mm-thick sample has higher D_s values than the other two samples. This result can be explained that the 2-mm-thick sample is too thin to produce much smoke while the 6 mm thick sample can form an effective residual char to prevent the production of combustible materials decomposed from the

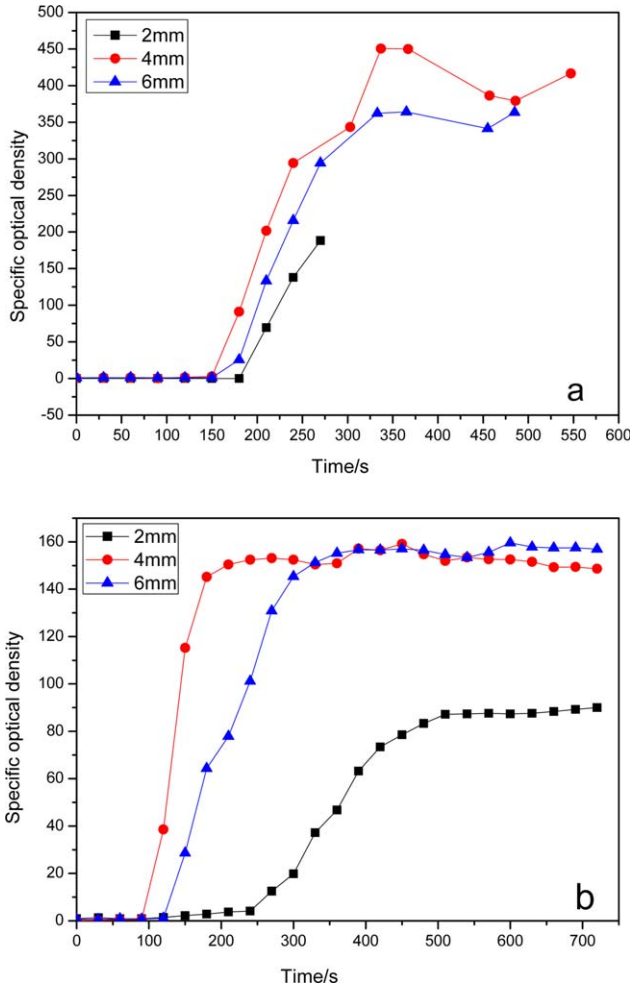

Figure 2. Specific optical density curves of EP/PA (a) and IFR-EP (b) at a flux of 25 kW m^{-2} with flame. [Color figure can be viewed in the online issue, which is available at wileyonlinelibrary.com.]

underlying materials; a similar phenomenon also appears in Figure 2(b).

Note that, all the IFR-EP samples have significantly lower values than the EP/PA samples, demonstrating that the IFR can effectively suppress smoke during the combustion process.

Dynamic Smoke Production Behaviors of EP/PA and IFR-EP

The cone calorimeter tests give detailed information about the dynamic smoke production behaviors of EP/PA and IFR-EP.

It can be seen from Figure 3, the smoke production rate (SPR) curves of EP/PA show multipeak phenomena, which tend to be more obvious with the sample thickness increase. Take the 6-mm-thick EP/PA sample for example, the SPR curve has a low and broad peak before 230 s, and then quickly reaches two high peaks. It can be explained that the epoxy crosslinked structure in EP/PA can contribute to the formation of char layer in early combustion stage; however, the initially formed char layer is not strong enough to retard the continuous combustion, and then, the protective char layer gradually decomposes as the sample is continuously exposed to the heat from cone.

However, with regard to the 6-mm-thick IFR-EP sample, the SPR curve reaches two high peaks first, and then shows a low and broad peak, suggesting that the epoxy crosslinked structure in IFR-EP can still contribute to the formation of char layer in the early combustion stage; moreover, the IFR can promote to form a more stable intumescent char layer in late combustion stage, which can significantly suppress smoke.

Figure 4 gives the SPR curves of EP/PA and IFR-EP under same test condition. Obviously, the sample containing IFR has much lower SPR values than EP/PA during almost the whole combustion process; however, in the early 30 s, the SPR values of IFR-EP are a little higher than that of EP/PA, indicating that the epoxy crosslinked structure in EP/PA can enhance the thermal stability and suppress smoke in the early combustion stage. Hence, it can be inferred that the epoxy crosslinked structure in IFR-EP can also exert its good thermal stability and smoke suppression properties. The thermal stability and smoke suppression properties of EP/PA and IFR-EP in the early combustion stage will be further revealed through a discussion of the mass loss, as shown in Figure 5.

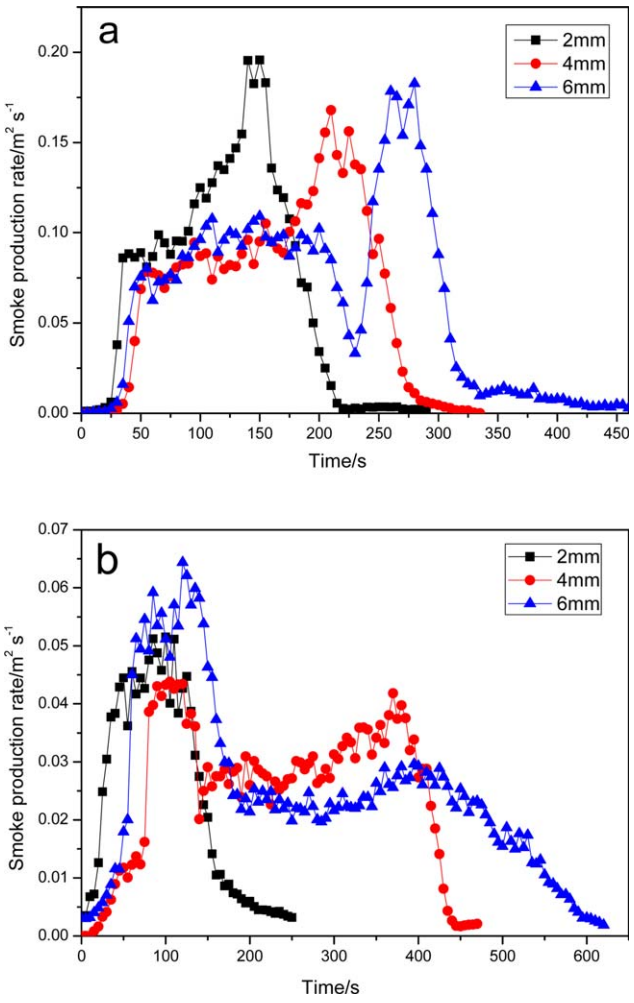

Figure 3. SPR curves of EP/PA (a) and IFR-EP (b) at a flux of 50 kW m^{-2}. [Color figure can be viewed in the online issue, which is available at wileyonlinelibrary.com.]

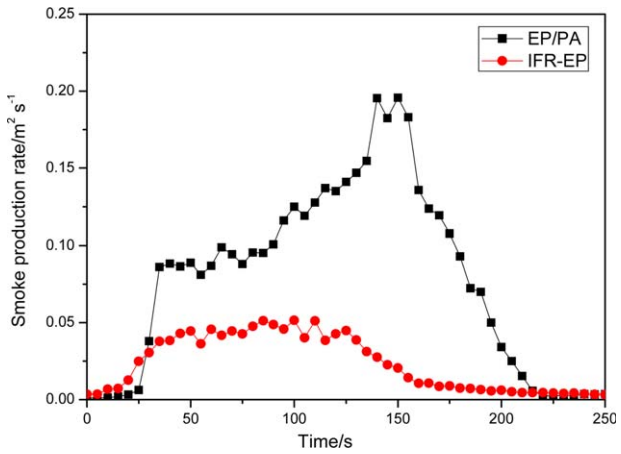

Figure 4. SPR curves of EP/PA and IFR-EP at a flux of 50 kW m^{-2}. [Color figure can be viewed in the online issue, which is available at wileyonlinelibrary.com.]

After ignition, the IFR-EP quickly loses its weight; while the EP/PA loses its weight at a much slower rate until 150 s. However, after 150 s the IFR-EP has a slower mass loss rate, and the char residue value of IFR-EP is higher than that of EP/PA.

These results reveal that the epoxy crosslinked structure in EP/PA can promote to form a stable and effective char layer to improve the thermal stability and suppress smoke in the early combustion stage, while the IFR tends to decompose at low temperature and then creates an excellent protective char barrier at high temperature to retard heat and suppress smoke.

To get more information about the dynamic smoke production behaviors of EP/PA and IFR-EP, more typical data from cone calorimeter tests are summarized in Table I. Each parameter has its own physical meaning, which represents the smoke suppression property and fire retardancy from a specific angle; hence, the combination of these data will give us full knowledge on the dynamic smoke production behaviors of EP/PA and IFR-EP.

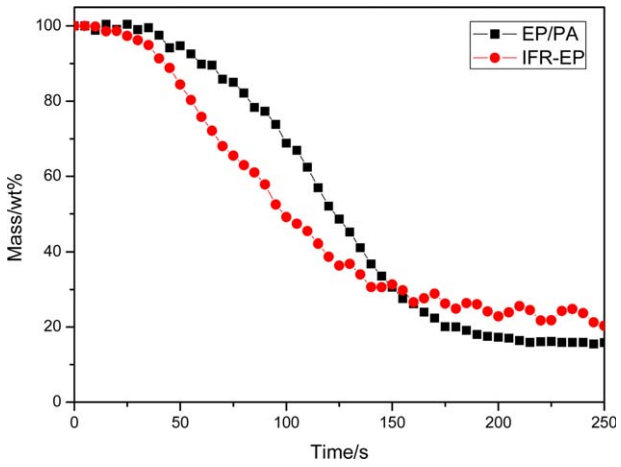

Figure 5. Mass loss curves of EP/PA and IFR-EP at a flux of 50 kW m^{-2}. [Color figure can be viewed in the online issue, which is available at wileyonlinelibrary.com.]

Table I. Typical Data of EP/PA and IFR-EP from Cone Calorimeter Tests

Resin	EP/PA	IFR-EP
PHRR (kW m^{-2})	1155.19	371.38
PSPR (m^2 s^{-1})	0.20	0.05
TSR (m^2 m^{-2})	2258.92	672.21
SEA_{av} (m^2 kg^{-1})	632.48	318.49
SF (MW m^{-2})	2609.48	249.65
SP (MW kg^{-1})	730.63	15.55

Among the data in Table I, the peak heat release rate (PHRR) refers to the risk of materials catching fire; the peak smoke production rate (PSPR) and total smoke rate (TSR) are the most important parameters, which represent the intensity of smoke production under the test conditions.

What's more, the smoke factor (SF) and the smoke parameter (SP) are also two important parameters: the SF represents a ratio of exhaust opacity to the amount of fuel burned at the time of measurement while the SP refers to the PHRR multiplied by average specific extinction area (SEA_{av}), and it gives an indication of the amount of smoke that would be generated during a full-scale fire.[27,28] Then, the two parameters can be calculated using eqs. (1) and (2):

$$SF = PHRR \times TSR \quad (1)$$

$$SP = SEA_{av} \times PHRR \quad (2)$$

Obviously, the lower the values of the two parameters are, the less smoke will be released.

Table I shows that the PHRR, PSPR, TSR, SEA_{av}, SF, and SP values of IFR-EP are much lower than that of EP/PA. All these data demonstrate that the IFR can efficiently reduce the risk of fire.

To get more information about fire hazards, the fire performance index (FPI) and the fire growth index (FGI) are calculated according to eqs. (3) and (4) after cone calorimeter test.

$$FPI = \frac{t_{ig}}{PHRR} \quad (3)$$

$$FGI = \frac{PHRR}{t_p} \quad (4)$$

The FPI (s m^2 kW^{-1}) represents the ratio of time to ignition (TTI or t_{ig}) and PHRR. A lower FPI value means the time to catching flashover is shorter and the fire risk is higher. The FGI (kW m^{-2} s^{-1}) represents the ratio of PHRR and time to PHRR (TTP or t_p). The FGI reflects the fire development speed; the higher the FGI value is, the shorter the time to PHRR will be, so the fire risk will be higher.[29,30] In other words, high FPI and low FGI values make the safety rank of materials high. From Figure 6, we can see that the IFR-EP has higher FPI and lower FGI values which indicate that it has higher safety rank than EP/PA.

Smoke Suppression Mechanism of EP/PA and IFR-EP

To confirm the above guesses, the TG and DTG analyses of EP/PA and IFR-EP were done for comparison; the corresponding curves are supplied in Figure 7 and the corresponding characteristic

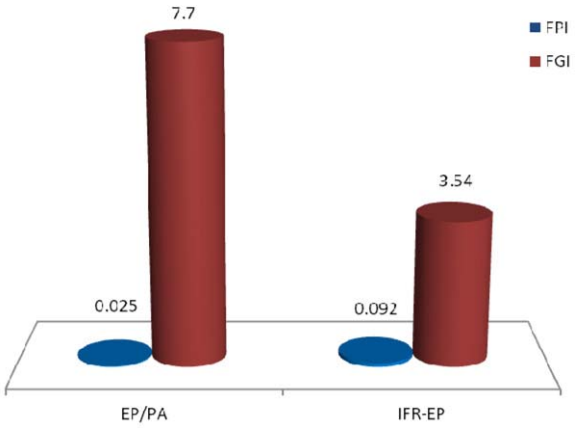

Figure 6. FPI and FGI for EP and IFR-EP at a flux of 50 kW m^{-2}. [Color figure can be viewed in the online issue, which is available at wileyonlinelibrary.com.]

parameters, such as the initial degradation temperature (T_d) considered as the temperature at which the mass loss of the sample reaches 5 wt %, the temperature at the maximum degradation rate (T_{max}) and char yield (Y_c) at 700 °C, are summarized in Table II.

Among the data in Table II, the T_d, T_{max1}, and T_{max2} values of IFR-EP are lower than that of EP/PA, demonstrating that the IFR system will decompose at lower temperatures while the epoxy crosslinked structure in EP/PA has greater ability to maintain the thermal stability in the early thermal degradation process. However, the thermal degradation of IFR will contribute to the formation of intumescent char, which can retard heat and suppress smoke effectively.

According to char yield at 700 °C, it can be seen that the IFR-EP has a greatly higher Y_c value than EP/PA; hence, the IFR can promote the formation of more stable char layer at high temperature.

Pyrolysis Gas Products of EP/PA and IFR-EP

In many cases of real fire hazards, most fire deaths are due to the toxic gases and oxygen deprivation[31]; therefore, it is important to

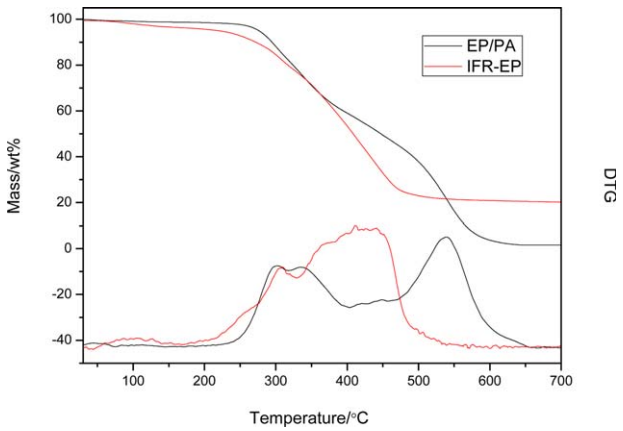

Figure 7. TG and DTG curves of EP/PA and IFR-EP under an air atmosphere. [Color figure can be viewed in the online issue, which is available at wileyonlinelibrary.com.]

Table II. Characteristic Data from TG Analyses under an Air Atmosphere

Sample	T_d (°C)	T_{max1} (°C)	T_{max2} (°C)	Y_c (wt %)
EP/PA	276.6	302.4	539.3	1.6
IFR-EP	220.9	104.9	411.5	20.1

discuss the pyrolysis gas products of EP/PA and IFR-EP. The TGA-FTIR spectra further disclose the pyrolysis information so that we can infer the main compositions of gas products in the thermal degradation process, and then get a deep insight into the smoke suppression mechanism of epoxy crosslinked structure and IFR.

Figure 8 shows the TGA-FTIR spectra of EP/PA and IFR-EP. The wavenumber range of 4000–3400 cm^{-1} and 2060–1260 cm^{-1} is assigned to the absorption peak of H_2O, the wavenumber range of 3100–2600 cm^{-1} is assigned to the absorption peak of CO_2, and the wavenumber range of 2260–1990 cm^{-1} is assigned to the absorption peak of CO. Obviously, the main gas products including H_2O, CO_2, and CO can be detected over the whole degradation

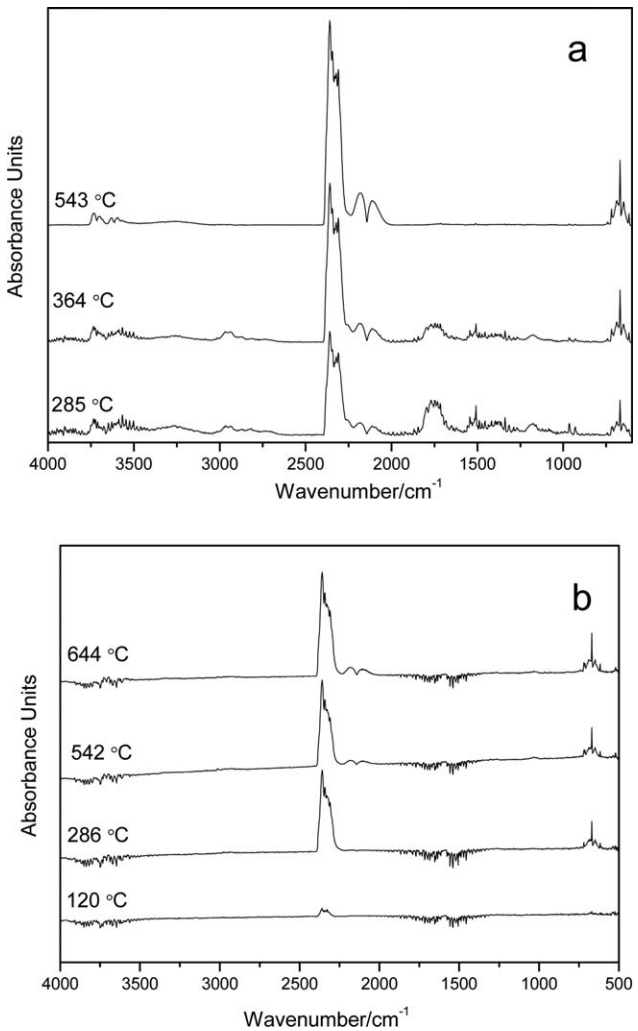

Figure 8. FTIR spectra of pyrolysis gas products of EP/PA (a) and IFR-EP (b) at different temperatures.

process of both EP/PA and IFR-EP. However, the carbonyl compound (1680–1750 cm^{-1}) and alkane (2853–2962 cm^{-1}) can only be found in the gas products of EP/PA.

Specifically, although the epoxy crosslinked structure in EP/PA can enhance the thermal stability and suppress smoke in the early combustion stage, it tends to be destroyed by the heat, and some harmful gas (C_3H_6O) and inflammable gas (CH_4) will be released from 285 to 364 °C, as shown in Figure 8(a). From Figure 8(b), the APP in IFR system usually decomposes at low temperature so that the absorption peak of H_2O and CO_2 can be detected at 120 °C. When the temperature reaches over 286 °C, the MEL and PER in IFR system begin to decompose, so the absorption peaks of H_2O and CO_2 are quite strong. When the temperature is over 542 °C, the intumescent char layer gradually loses its protective effect so that the absorption peaks of H_2O, CO_2, and CO become more and more obvious.

These results suggest that the epoxy crosslinked structure in EP/PA can only exert its smoke suppression effect at low temperature while the IFR can effectively reduce the production of toxic and inflammable gases just as acetone and alkane derived from EP/PA at high temperature.

Based on the above discussions, it is reasonable to conclude that the crosslinked structure in EP/PA can strengthen the thermal stability and suppress smoke in the early combustion stage, and the intumescent char derived from IFR will effectively retard heat and suppress smoke in late combustion stage.

CONCLUSIONS

EP/PA is a kind of outstanding film former for IFR-EPs. The epoxy crosslinked structure in EP/PA can enhance the thermal stability and suppress smoke in the early combustion stage; while the IFR can promote the smoke suppression and reduce the production of toxic and inflammable gases during combustion. The superior smoke production behaviors of epoxy crosslinked structure and IFR in IFR-EP endow the IFR-EP with perfect smoke suppression properties.

ACKNOWLEDGMENTS

The authors gratefully acknowledge the financial support of National Natural Science Foundation of China (No. 51006054) and Shandong Provincial Natural Science Foundation of China (ZR2014EEM037).

REFERENCES

1. Lu, H. D.; Song, L.; Hu, Y. *Polym. Adv. Technol.* **2011**, *2*, 379.
2. Nakka, J. S.; Jansen, K. M. B.; Ernst, L. J. *J. Appl. Polym. Sci.* **2013**, *128*, 3794.
3. Levchik, S.; Weil, E. *Polym. Int.* **2004**, *53*, 1901.
4. Chen, X. L.; Jiao, C. M.; Li, S. X.; Sun, J. *J. Polym. Res.* **2011**, *18*, 2229.
5. Zhang, D. H.; Jia, D. J.; Chen, S. F. *J. Therm. Anal. Calorim.* **2009**, *98*, 819.
6. Ricciardi, M. R.; Antonucci, V.; Zarrellim, M.; Giordano, M. *Fire Mater.* **2012**, *36*, 203.
7. Jiao, C. M.; Zhuo, J. L.; Chen, X. L.; Li, S. X.; Wang, H. J. *J. Therm. Anal. Calorim.* **2013**, *114*, 253.
8. Liu, Q.; Bao, X.; Deng, S. Q.; Cai, X. *J. Therm. Anal. Calorim.* **2014**, *118*, 247.
9. Wu, X. F.; Wang, L. C.; Wu, C.; Yu, J. H.; Xie, L. Y.; Wang, G. L.; Jiang, P. K. *Polym. Degrad. Stabil.* **2012**, *97*, 54.
10. Gu, J. W.; Zhang, G. C.; Dong, S. L.; Zhang, Q. Y.; Kong, J. *Surf. Coat. Technol.* **2007**, *201*, 7835.
11. Guo, T.; Labelle, B.; Petreas, M.; Park, J. S. *Rapid Commun. Mass Spectrom.* **2013**, *27*, 1437.
12. Hartzell, G. E.; Priest, D. N.; Switzer, W. G. *J. Fire Sci.* **1985**, *3*, 115.
13. Kim, S. *J. Polym. Sci. Part B: Polym. Phys.* **2003**, *41*, 936.
14. Li, G. X.; Wang, W. J.; Cao, S. K.; Cao, Y.; Wang, J. *J. Appl. Polym. Sci.* **2014**, *131*, DOI: 10.1002/app.40054.
15. Waaijers, S. L.; Kong, D.; Hendriks, H. S.; de Wit, C. A.; Cousins, I. T.; Westerink, R. H.; Leonards, P. E.; Kraak, M. H.; Admiraal, W.; de Voogt, P.; Parsons, J. R. *Rev. Environ. Contam.* **2013**, *222*, 1.
16. Delmas, G. H.; Benjelloun-Mlayah, B.; Bigot, Y. L.; Delmas, M. *J. Appl. Polym. Sci.* **2003**, *127*, 1863.
17. Lebel, L. S.; Brousseau, P.; Erhardt, L.; Andrews, W. S. *Combust. Flame* **2014**, *161*, 1038.
18. Qu, H. Q.; Wu, W. H.; Hao, J. W.; Wang, C.; Xu, J. *Fire Mater.* **2014**, *38*, 31.
19. Lin, G. P.; Chen, L.; Wang, X. L.; Jian, R. K.; Zhao, B.; Wang, Y. Z. *Ind. Eng. Chem. Res.* **2013**, *52*, 15613.
20. Zhao, J.; Deng, C. L.; Du, S. L.; Chen, L.; Deng, C.; Wang, Y. Z. *J. Appl. Polym. Sci.* **2014**, *131*, DOI: 10.1002/app.40065.
21. Lai, X. J.; Zeng, X. R.; Li, H. Q.; Zhang, H. *J. Macromol. Sci. B* **2014**, *53*, 721.
22. Chen, X. Y.; Sun, T.; Cai, X. F. *J. Therm. Anal. Calorim.* **2014**, *115*, 185.
23. Chonkaew, W.; Sombatsompop, N. *J. Appl. Polym. Sci.* **2012**, *125*, 361.
24. Chen, K. S.; Yeh, R. Z. *J. Hazard. Mater.* **1996**, *49*, 105.
25. Mulholland, G. W. Handbook of Fire Protection Engineering; NFPA: Quincy, MA, **2008**.
26. Sun, Y. Y.; Zhang, F.; Wang, W. T.; Yu, J. *Modern Plastics Proc Appl* **2013**, *25*, 6.
27. Han, J. P.; Liang, G. Z.; Gu, A.; Ye, J.; Zhang, Z.; Yuan, L. *J. Mater. Chem. A* **2013**, *1*, 2169.
28. Chen, X. L.; Jiang, Y. F.; Jiao, C. M. *J. Hazard. Mater.* **2014**, *266*, 114.
29. Cogen, J. M.; Lin, T. S.; Lyon, R. E. *Fire Mater.* **2009**, *33*, 33.
30. Wang, D.; Zhang, Q.; Zhou, K.; Yang, W.; Hu, Y.; Gong, X. L. *J. Hazard. Mater.* **2014**, *278*, 391.
31. Gann, R. G.; Babrauskas, V.; Peacock, R. D.; Hall, J. R. *Fire Mater.* **2004**, *18*, 193.